AIP | Applied Physics Letters

# Realization of unbiased photoresponse in amorphous InGaZnO ultraviolet detector via a hole-trapping process

D. L. Jiang, L. Li, H. Y. Chen, H. Gao, Q. Qiao, Z. K. Xu, and S. J. Jiao

Citation: Applied Physics Letters **106**, 171103 (2015); doi: 10.1063/1.4918991
View online: http://dx.doi.org/10.1063/1.4918991
View Table of Contents: http://scitation.aip.org/content/aip/journal/apl/106/17?ver=pdfcov
Published by the AIP Publishing



# Realization of unbiased photoresponse in amorphous InGaZnO ultraviolet detector via a hole-trapping process

D. L. Jiang,[1] L. Li,[1,a)] H. Y. Chen,[2] H. Gao,[1] Q. Qiao,[3] Z. K. Xu,[1] and S. J. Jiao[4]
[1]*Key Laboratory for Photonic and Electronic Bandgap Materials, Ministry of Education, School of Physics and Electronic Engineering, Harbin Normal University, Harbin 150025, People's Republic of China*
[2]*State Key Laboratory of Luminescence and Applications, Changchun Institute of Optics, Fine Mechanics and Physics, Chinese Academy of Sciences, Dongnanhu Road 3888, Changchun 130033, People's Republic of China and Graduate University of the Chinese Academy of Sciences, Beijing 100049, People's Republic of China*
[3]*School of Naval Architecture and Ocean Engineering, Zhejiang Ocean University, Zhoushan 316000, People's Republic of China*
[4]*School of Materials Science and Engineering, Harbin Institute of Technology, Harbin 150001, People's Republic of China*

(Received 7 December 2014; accepted 12 April 2015; published online 27 April 2015)

A metal-semiconductor-metal (MSM) structure ultraviolet photodetector has been fabricated from amorphous InGaZnO (a-IGZO) film at room temperature. The photodetector can work without consuming external power and show a responsivity of 4 mA/W. The unbiased photoresponse characteristic is attributed to the hole-trapping process occurred in the electrode/a-IGZO interface, and a physical model based on band energy theory is proposed to explain the origin of the photoresponse at zero bias in our device. Our findings may provide a way to realize unbiased photoresponse in the simple MSM structure. © *2015 AIP Publishing LLC*. [http://dx.doi.org/10.1063/1.4918991]

Ultraviolet (UV) photodetectors (PDs) have drawn increasing attention due to their potential applications in air-pollution/waste-water monitoring, missile plume detection, flame alarm, and secure communication.[1–4] From the application and energy saving point of view, the PDs working without consuming external power are very important. For example, the UV PDs operating without any power supply are highly desired for unattended, long-term monitoring air-pollution and wastewater.[1] Thus, they have recently received increasing attention. Untill now, UV PDs working at zero bias based on GaN, ZnO, and $TiO_2$[5–7] have been realized by *pn* junction, heterojunction, and Schottky junction, owing to their efficient separation of photo-generated electron-hole pairs using photovoltaic effect. However, there are still some problems in these UV PDs working at zero bias. Most of these semiconductor films require a high growth temperature (>300 °C),[8–11] complicated preparation process, which will increase manufacturing cost of devices. Moreover, the lack of high quality and stable *p*-type semiconductors (such as ZnO), large lattice mismatch in heterojunctions will introduce a large number of dislocations and their associated point defects,[12] which will degrade greatly the performance of the device. Therefore, the realization of a UV PD working at zero bias, which can avoid the above problems, is urgently needed.

Amorphous InGaZnO (a-IGZO) film has attracted much attention due to its great potential in optoelectronic applications such as transparent thin film transistors (especially on flexible substrates),[13,14] phototransistor,[15–17] and so on. Benefiting from superior features over other semiconductors including room temperature (RT) process availability, good-uniformity for large area, wide band gap (>3.0 eV), and high electron mobility (1–30 $cm^2/V$ s at RT),[18–21] it has also been used to fabricate UV detectors.[22,23] However, the structure of the reported a-IGZO UV detectors is focused on the transistor structure which need a complicated fabrication process. Particularly, metal-semiconductor-metal (MSM) photodiodes are a family of fast, high-sensitivity detectors. Their simple planar structures enable easy fabrication in a process compatible with planar circuit technology. Thus, these devices are attractive candidates for using in integrated optoelectronic-electronic systems. If a UV detector working at zero bias based on simple MSM structure fabricated at RT was realized, then it will have extensive commercial applications. Till now, an a-IGZO UV detector working at zero bias based on simple MSM structure has not been reported yet.

In this paper, a-IGZO UV PD has been fabricated based on MSM structure at RT, which can operate without an external power supply. The origin of its unbiased photoresponse characteristic is studied in detail. The hole-trapping process occurred in metal electrode/a-IGZO interface play an important role in realization of the unbiased photoresponse of a-IGZO UV PD. It may provide an insight to obtain a UV PD working at zero bias based on simple MSM structure.

The IGZO film employed for the active layer of the UV detector was grown on *c*-plane sapphire substrate by plasma-assisted pulsed laser deposition technique using a Nd:YAG pulsed laser (Quantel Brilliant B). The cleaning process of the sapphire can be found in our previous publication.[24] Prior to growth, the growth chamber was pumped to a base pressure below $6.0 \times 10^{-5}$ Pa with a turbo molecular pump. High purity oxygen gas (99.99%) was introduced into the growth chamber, and it was activated by a high voltage ionization equipment (voltage: 0.45 kV). The oxygen flow was fixed at 20 sccm, the pressure in the growth chamber

a)Electronic mail: physics_lin@hotmail.com

 

was maintained at 5.0 Pa, and a Nd:YAG pulsed laser ($\lambda = 355$ nm, $t_s = 5$ ns, repetition rate = 10 Hz, laser energy: 170 mJ/pulse) was employed to ablate IGZO target (purity > 99.99%, In:Ga:Zn = 1:1:1) during the growth process. The IGZO film was deposited at RT for 2 h. To fabricate the IGZO UV PD, an Au film of 60 nm was evaporated onto the IGZO film by the vacuum thermal evaporation technique. The interdigital electrodes were configured onto the IGZO layer through the photolithography and wet etching process.

The morphology of the IGZO film was characterized using a Hitachi SU70 scanning electron microscope (SEM). The Hall measurement system was used to check the electrical properties of the IGZO film. X-ray diffractometer (XRD) was employed to evaluate the crystalline properties of the IGZO film. The optical absorption spectrum of the IGZO layer was recorded with an ultraviolet-visible spectrophotometer. The current-voltage (*I-V*) characteristic of the device was obtained from the Agilent B1500A semiconductor device analyzer. The responsivity (Zolix DR800-CUST) characteristics of the MSM structure a-IGZO PD were measured at RT. The temporal response of the PD was measured by an Nd:YAG pulsed laser (266 nm, 10 ns) as the excitation source.

Fig. 1(a) shows the XRD pattern of the IGZO film grown on *c*-sapphire. Besides the diffraction from the sapphire substrate,[25] there is no other obvious peak in the pattern, indicating the IGZO film is amorphous.[26] The surface morphology and cross sectional of the a-IGZO film is shown in Fig. 1(b). Nanoparticles with average diameter of about 50 nm are observed from the SEM image of the a-IGZO film. The thickness of the film is 180 nm, which is shown in the inset of Fig. 1(b). The optical absorption spectrum of the a-IGZO film is shown in Fig. 1(c), which exhibits a strong UV absorption. Fig. 1(d) shows the photoresponse characteristic of the PD under illumination condition at zero bias. It can be found that the responsivity of the PD is 4 mA/W, and the peak response wavelength is located at 310 nm. The above photoresponse at zero bias indicates that an asymmetric Schottky barrier is formed at two electrode/a-IGZO interfaces. Structure of the device is schematically shown in Fig. 2(d). The MSM structure a-IGZO PD consists of 12 pairs of interdigital Au electrodes, each finger is 500 $\mu$m in length, 5 $\mu$m in width, and the spacing between fingers is 10 $\mu$m. The electrodes at the two sides of the interdigital are named $M_1$ and $M_2$ for simplicity, respectively.

To investigate the origin of the unbiased photoresponse in the PD, a series of bias voltages have been applied onto the UV PD, and the spectral responsivity was recorded, as shown in Fig. 2(a) and 2(b). Comparing Fig. 2(a) with Fig. 2(b), one can find that the peak response wavelength of the PD is located at 310 nm from 0 V to 10 V when the forward bias is applied on the PD from $M_1$ to $M_2$ (named forward bias in Fig. 2(a)). However, when the reverse bias is applied on the PD from $M_1$ to $M_2$ (named reverse bias in Fig. 2(b)), the peak response wavelength exhibits a gradual blueshift from 310 nm to 300 nm at 0 V to −10 V. The blueshift of the peak response wavelength with the reverse bias increasing has been observed in Schottky detectors.[27] It can be explained as below. The electric field of the depletion region will be increased as the bias between two electrodes increasing, the transit time of photo-induced carriers drifting across the depletion region will be shorten, thus, the carriers induced by absorption of shorten wavelength photons will pass through the depletion region prior to recombination. However, the blueshift of peak response wavelength can only be observed under reverse bias in our PD, which indicates the blueshift cannot be attributed to the increase of external bias. Fig. 2(c) illustrates the responsivity of the PD as a function of a series of bias applied at two electrodes

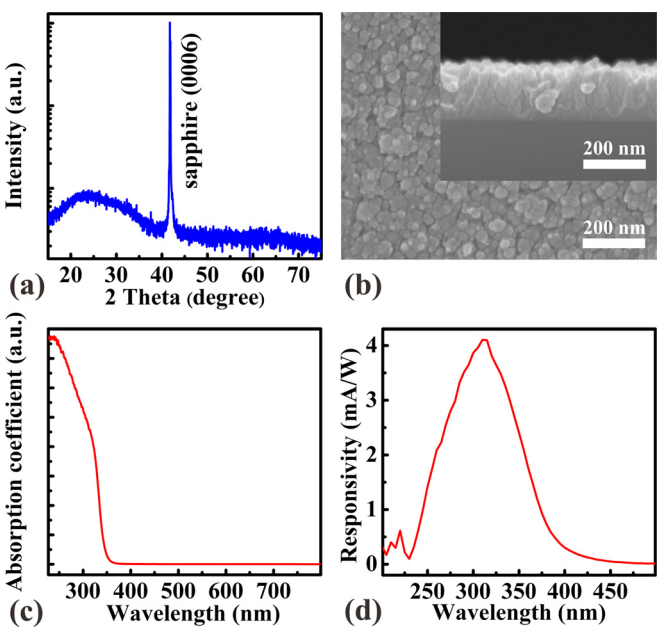


FIG. 1. (a) XRD pattern of the as-grown IGZO film. (b) The top-view and cross-sectional (inset) SEM images of the a-IGZO film. (c) The optical absorption spectrum of the a-IGZO film. (d) The photoresponse characteristic of the MSM structure a-IGZO photodetector at 0 V bias.

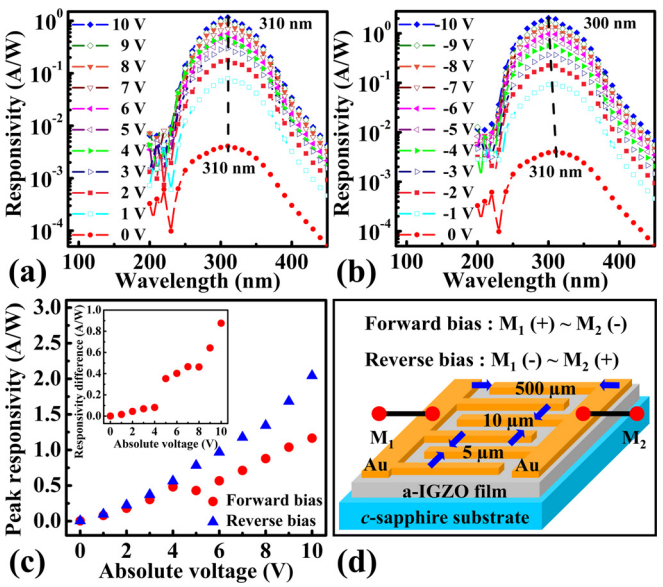


FIG. 2. The photoresponse spectra of the a-IGZO photodetector as a function of the incident light wavelength under different: (a) forward bias and (b) reverse bias. (c) The responsivity of the detector under each absolute value of forward (red spot) or reverse (blue triangle) bias, and the inset shows the responsivity difference of the PD at the same absolute bias. (d) The schematic diagram of the MSM structure a-IGZO detector.

(forward bias and reverse bias). It is obvious that the responsivity almost changes linearly with the forward bias increasing. However, the responsivity exhibits a nonlinear increase with the reverse bias increasing. To further demonstrate the difference of responsivity under forward and reverse bias, the inset of Fig. 2(c) shows the difference of responsivity under the same absolute bias (that is, the responsivity of the PD at reverse bias minus the responsivity of the PD at forward bias), it can be clearly seen that the difference of responsivity increases with the absolute bias increasing, which indicates that another internal mechanism should be responsible for the blueshift of peak response wavelength and improvement of responsivity in the PD under reverse bias.

To explore the origin of the internal mechanism, the current-voltage (*I-V*) characteristic of the PD measured in dark is shown in Fig. 3(a). The *I-V* curve shows a clear Schottky behavior, which comes from the Au/a-IGZO interfaces. Furthermore, an obvious asymmetric shape in the positive and negative voltage regions can be observed in the *I-V* curve of Fig. 3(a). In order to better understand the carrier transportation process at the Au/a-IGZO interfaces, one must identify which transport process plays a dominant role in our PD. In general, for a Schottky contact, if $E_{00} \gg k_B T$, the thermionic emission will dominate the carrier transportation process without tunneling, where $k_B$ is the Boltzmann constant, and $T$ is the absolute temperature. $E_{00}$ can be described as follows: $E_{00} = (\hbar q/2)(N/m^* \varepsilon_r)^{1/2}$. $E_{00}$ is the characteristic energy related to the tunneling probability, $\hbar$ is the reduced Planck constant, $q$ is the elementary charge, $N$ is the carrier density in the semiconductor, $m^*$ is the effective mass, and $\varepsilon_r$ is the relative dielectric permittivity. In our case, the $m^* = 0.34 m_0$,[28] $N = 1.77 \times 10^{16}$ cm$^{-3}$ by hall measurement, $\varepsilon_r = 10$,[17] $E_{00}$ is about 0.73 meV for the a-IGZO film, which is smaller than the thermal energy at RT (26 meV). Therefore, the thermionic emission will be employed to analyze the carrier transport process in our case.

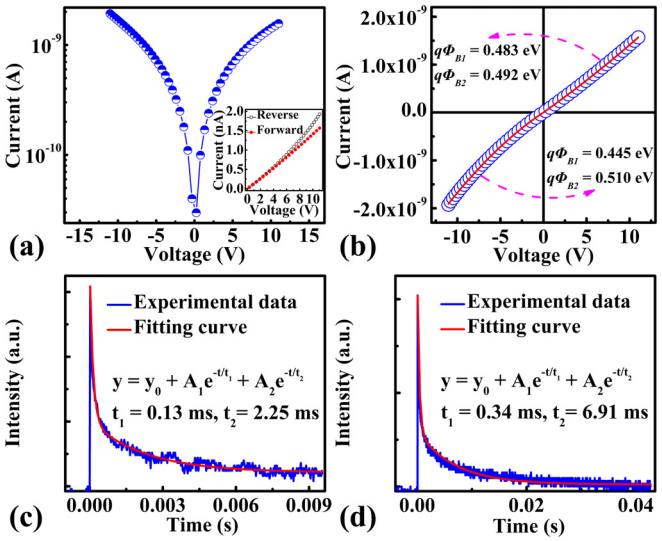


FIG. 3. (a) The *I-V* characteristic of the a-IGZO photodetector measured in dark. Inset: the *I-V* curve in first quadrant. (b) Fitting results of the *I-V* curve of the detector, in which the scattered blue open circles are experimental data, while the red solid line is a fitting of the experimental data. (c) and (d) The temporal response of the a-IGZO photodetector at voltage of +5 V (c) and −5 V (d).

Based on thermionic emission model, the current passing through the Schottky barrier can be expressed by the following formula: $I = I_0[\exp(qV/nkT) - 1]$, where $I_0$ is the saturation current; it can be described as follows: $I_0 = A_1 A_n^* T^2 \exp(-q\phi_B/k_B T)$, $q$ is the elementary charge, $V$ is the applied bias, and $n$ is the ideality factor, $A_1$ is the junction area, $A_n^*$ is the Richardson constant ($A_n^* = 4\pi m^* q^2/h^3$), which is 41 A cm$^{-2}$ K$^{-2}$ for a-IGZO film,[29] and $\phi_B$ is the Schottky barrier height.

In our case, the MSM structure consists of two Schottky barriers connected back to back on a coplanar surface, the current in the PD as a function of applied bias voltage can be described as follows:[30]

$$I = I_1\left[\exp\left(\frac{qV}{nk_BT}\right) - 1\right] + I_2\left[\exp\left(\frac{qV}{nk_BT}\right) - 1\right], \quad (1)$$

where $I_1 = A_1 A_n{}^* T^2 \exp(-\frac{q\phi_{B1}}{k_B T})$, $I_2 = A_1 A_n{}^* T^2 \exp(-\frac{q\phi_{B2}}{k_B T})$, $\phi_{B1}$ and $\phi_{B2}$ are the Schottky barrier height at the two sides of the interdigital electrodes, respectively. By fitting the *I-V* curve using the Eq. (1), one can obtain the Schottky barrier height at the two sides of the interdigital electrodes. The fitting result is shown in Fig. 3(b). At forward bias, the two Schottky barriers have little difference ($q\phi_{B1} = 0.483$ eV at $M_1$ electrode and $q\phi_{B2} = 0.492$ eV at $M_2$ electrode); however, an obvious asymmetric Schottky barrier is observed at negative bias ($q\phi_{B1} = 0.445$ eV at $M_1$ electrode and $q\phi_{B2} = 0.510$ eV at $M_2$ electrode). So, the origin of the asymmetric Schottky barrier formed under reverse bias should be the internal mechanism of blueshift of peak response wavelength and improvement of responsivity in our PD under reverse bias. The asymmetric Schottky barrier was also found in ZnO MSM detectors, which is attributed to the carrier-trapping process occurred in electrode/ZnO interface.[30] The trap states may come from the surface damaging during the device processing or the interface states associated with grain boundary defects.[31] In our case, the asymmetric Schottky barrier is mainly formed under reverse bias, and it should be understood as below: Under reverse bias, the photo-generated holes are accumulated in the $M_1$/a-IGZO interface and trapped by the trap states, which will modify the localized potential profile, so the effective height of the Schottky barrier is lowered at $M_1$/a-IGZO interface compare to the Schottky barrier at $M_2$/a-IGZO interface.[32–34] However, the two Schottky barriers show a little difference under forward bias, which indicate the trap states mainly exist in the $M_1$/a-IGZO interface. The asymmetry trapping states at two Au/a-IGZO interfaces may originate from the non-uniform properties of the a-IGZO film or the electrodes in our case.

Figs. 3(c) and 3(d) show the temporal response of the PD at ±5 V bias. The response time is about 14.7 $\mu$s (+5 V) and 15.4 $\mu$s (−5 V), respectively, which is estimated as the 10%–90% rise time. The decay edge can be well fitted by a two-order exponential decay fomula;[35] it can be seen that the carrier lifetime at −5 V bias is obviously larger than that at +5 V bias ($t_1 = 0.13$ ms, $t_2 = 2.25$ ms at +5 V bias in Fig. 3(c); $t_1 = 0.34$ ms, $t_2 = 6.91$ ms at −5 V bias in Fig. 3(d)), which illustrates the lifetime of photo-generated carriers of

the PD is longer under reverse bias, owing to more holes trapped by the interface trap states in $M_1$/a-IGZO interface.

Based on above experimental results and analysis, a reasonable model was proposed as shown in Fig. 4 in terms of energy band theory. Under UV illumination, electron-hole pairs are generated in the a-IGZO film. As the reverse bias increasing in our PD, the electric field of the depletion region is gradually enhanced, then more and more holes are quickly transported to the $M_1$/a-IGZO interface before recombination, and bounded to the trap states (as shown in Fig. 4(a)), then recombination rate of photo-generated electron-hole pairs will be decreased, especially for the electron-hole pairs generated by the absorption of the short-wavelength photons, which will extend the lifetime of excess carriers. It is well known that the high responsivity could be obtained when the lifetime of the photo-generated carriers is longer than the transport time between $M_1$ and $M_2$ electrodes.[36] While a forward bias is applied from $M_1$ to $M_2$, the photo-generated holes will accumulate in the $M_2$/a-IGZO interface, only a small amount of holes will be trapped by the few number of trap states in the $M_2$/a-IGZO interface (as shown in Fig. 4(b)), so the recombination effect of photo-generated electron-hole pairs will be more serious at forward bias than that at the condition of reverse bias. Therefore, the blueshift of the peak response wavelength and enhancement of responsivity of PD is only observed under reverse bias. Based on above analysis, the photoresponse at 0 V in our PD is attributed to the hole-trapping process occurred in the $M_1$/a-IGZO interface, and the energy band diagram of the PD at 0 V under UV illumination is displayed in Fig. 4(c).

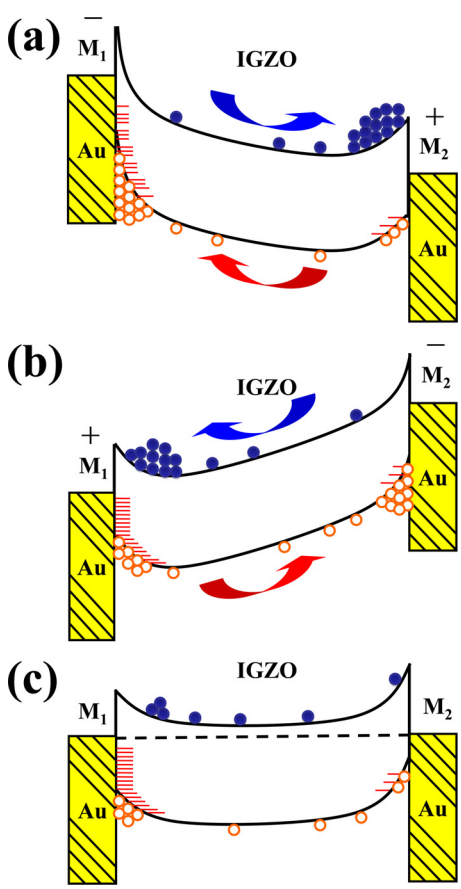


FIG. 4. Energy band diagrams of the MSM structure a-IGZO photodetector in UV light: (a) at reverse bias, (b) at forward bias, and (c) at 0 V bias.

In summary, a UV detector working at zero bias has been obtained from Au/a-IGZO MSM structure. The unbiased photoresponse characteristic is attributed to the hole-trapping process occurred in the $M_1$/a-IGZO interface, which has been confirmed by the responsivity characteristics of the PD and an asymmetric Schottky barrier formed at the two sides of the Au/a-IGZO interdigital electrodes under reverse bias. The results reported in the paper provide a possible way to realize detector working at zero bias in simple planar MSM structure via the hole-trapping process.

This work was supported by the Natural Science Foundation of China (Grant No. 61404039), Heilongjiang Province Foundation for Returned Chinese Scholars (Grant No. LC201401), the Youth Science Foundation of Heilongjiang Province (Grant No. QC2014C056), and Educational Commission of Heilongjiang Province of China (Grant No. 12531Z006).

[1]Q. Yang, Y. Liu, Z. T. Li, Z. Y. Yang, X. Wang, and Z. L. Wang, Angew. Chem. **124**, 6549 (2012).
[2]E. Monroy, F. Omnes, and F. Calle, Semicond. Sci. Technol. **18**, R33 (2003).
[3]G. M. Ail and P. Chakrabarti, J. Phys. D: Appl. Phys. **43**, 415103 (2010).
[4]J. Yu, C. X. Shan, X. M. Huang, X. W. Zhang, S. P. Wang, and D. Z. Shen, J. Phys. D: Appl. Phys. **46**, 305105 (2013).
[5]Y. Q. Bie, Z. M. Liao, H. Z. Zhang, G. R. Li, Y. Ye, Y. B. Zhou, J. Xu, Z. X. Qin, L. Dai, and D. P. Yu, Adv. Mater. **23**, 649 (2011).
[6]H. Shen, C. X. Shan, B. H. Li, B. Xuan, and D. Z. Shen, Appl. Phys. Lett. **103**, 232112 (2013).
[7]X. D. Li, C. T. Gao, H. G. Duan, B. A. Lu, X. J. Pan, and E. Q. Xie, Nano Energy **1**, 640 (2012).
[8]D. B. Li, X. J. Sun, H. Song, Z. M. Li, H. Jiang, Y. R. Chen, G. Q. Miao, and B. Shen, Appl. Phys. Lett. **99**, 261102 (2011).
[9]C. G. Tian, D. Y. Jiang, B. Z. Li, J. Q. Lin, Y. J. Zhao, W. X. Yuan, J. X. Zhao, Q. C. Liang, S. Gao, J. H. Hou, and J. M. Qin, ACS Appl. Mater. Interfaces **6**, 2162 (2014).
[10]J. Xing, H. Y. Wei, E. J. Guo, and F. Yang, J. Phys. D: Appl. Phys. **44**, 375104 (2011).
[11]X. H. Xie, Z. Z. Zhang, C. X. Shan, H. Y. Chen, and D. Z. Shen, Appl. Phys. Lett. **101**, 081104 (2012).
[12]J. Zou, D. J. H. Cockayne, and B. F. Usher, J. Appl. Phys. **73**, 619 (1993).
[13]M. J. Yu, Y. H. Yeh, C. C. Cheng, C. Y. Lin, G. T. Ho, B. C. M. Lai, C. M. Leu, T. H. Hou, and Y. J. Chan, IEEE Electron Device Lett. **33**, 47 (2012).
[14]S. Yang, J. Y. Bak, S. M. Yoon, M. K. Ryu, H. Oh, C. S. Hwang, G. H. Kim, S. H. K. Park, and J. Jang, IEEE Electron Device Lett. **32**, 1692 (2011).
[15]H. W. Zan, W. T. Chen, H. W. Hsueh, S. C. Kao, M. C. Ku, C. C. Tsai, and H. F. Meng, Appl. Phys. Lett. **97**, 203506 (2010).
[16]T. H. Chang, C. J. Chiu, S. J. Chang, T. Y. Tsai, T. H. Yang, Z. D. Huang, and W. Y. Weng, Appl. Phys. Lett. **102**, 221104 (2013).
[17]T. H. Chang, C. J. Chiu, W. Y. Weng, S. J. Chang, T. Y. Tsai, and Z. D. Huang, Appl. Phys. Lett. **101**, 261112 (2012).
[18]S. J. Liu, S. H. Su, and J. Y. Juang, Appl. Phys. A **116**, 1473 (2014).
[19]T. Kamiya, K. Nomura, and H. Hosono, J. Disp. Technol. **5**, 273 (2009).
[20]A. Suresh, P. Gollakota, P. Wellenius, A. Dhawan, and J. F. Muth, Thin Solid Films **516**, 1326 (2008).
[21]S. J. Liu, H. W. Fang, S. H. Su, C. H. Li, J. S. Cherng, J. H. Hsieh, and J. Y. Juang, Appl. Phys. Lett. **94**, 092504 (2009).
[22]T. C. Fung, C. S. Chuang, K. Nomura, H. P. D. Shieh, H. Hosono, and J. Kanicki, J. Inf. Disp. **9**, 21 (2008).
[23]J. Yao, N. Xu, S. Deng, J. Chen, J. She, H. P. D. Shieh, P. T. Liu, and Y. P. Huang, IEEE Trans. Electron Devices **58**, 1121 (2011).
[24]L. Li, C. X. Shan, S. P. Wang, B. H. Li, J. Y. Zhang, B. Yao, D. Z. Shen, X. W. Fan, and Y. M. Lu, J. Phys. D: Appl. Phys. **42**, 195403 (2009).
[25]W. W. Liu, B. Yao, Z. Z. Zhang, Y. F. Li, B. H. Li, C. X. Shan, J. Y. Zhang, D. Z. Shen, and X. W. Fan, J. Appl. Phys. **109**, 093518 (2011).

[26]K. Nomura, H. Ohta, A. Takagi, T. Kamiya, M. Hirano, and H. Hosono, Nature **432**, 488 (2004).
[27]S. M. Sze, *Semiconductor Devices: Physics and Technology* (John Wiley & Sons, 2008).
[28]A. Takagi, K. Nomura, H. Ohta, T. Kamiya, M. Hirano, and H. Hosono, Thin Solid Films **486**, 38 (2005).
[29]A. Chasin, E. Simoen, A. Bhoolokam, M. Nag, J. Genoe, G. Gielen, and P. Heremans, Appl. Phys. Lett. **104**, 082112 (2014).
[30]J. S. Liu, C. X. Shan, B. H. Li, Z. Z. Zhang, C. L. Yang, D. Z. Shen, and X. W. Fan, Appl. Phys. Lett. **97**, 251102 (2010).
[31]I. Shalish, L. Kronik, G. Segal, Y. Shapira, S. Zamir, B. Meyler, and J. Salzman, Phys. Rev. B **61**, 15573 (2000).
[32]Z. L. Wang, Adv. Mater. **24**, 4632 (2012).
[33]O. Katz, V. Garber, B. Meyler, G. Bahir, and J. Salzman, Appl. Phys. Lett. **79**, 1417 (2001).
[34]H. Y. Chen, K. W. Liu, X. Chen, Z. Z. Zhang, M. M. Fan, M. M. Jiang, X. H. Xie, H. F. Zhao, and D. Z. Shen, J. Mater. Chem. C **2**, 9689 (2014).
[35]P. N. Ni, C. X. Shan, S. P. Wang, X. Y. Liu, and D. Z. Shen, J. Mater. Chem. C **1**, 4445 (2013).
[36]G. Konstantatos and E. H. Sargent, Nat. Nanotechnol. **5**, 391 (2010).